

Classification
 Physics Abstracts
 03.20 — 05.45

Swinging Atwood's Machine : integrability and dynamics

J. Casasayas ^(1, *), A. Nunes ⁽²⁾ and N. Tufillaro ^(3, **)

⁽¹⁾ Departament de Matemàtica Aplicada i Anàlisi, Universitat de Barcelona, Spain

⁽²⁾ Departamento de Física, Universidade de Lisboa, Portugal

⁽³⁾ Department of Physics, Bryn Mawr College, U.S.A.

(Received on December 28, 1989, accepted in final form on April 25, 1990)

Abstract. — We consider the Swinging Atwood's Machine model (SAM) and show that it is non-integrable whenever the mass ratio μ is greater than 3. This solves negatively the conjecture, based in numerical experiments, that the SAM is integrable for $\mu = 4n^2 - 1$, $n \in \mathbb{N}$. We study the transversal heteroclinic orbits of the system and explain why does the system «look» integrable for these values of μ .

1. Introduction.

The Swinging Atwood's machine (SAM) is a two degrees of freedom Hamiltonian system depending on a real parameter $\mu \in [0, +\infty)$ that corresponds to a very simple physical model (see Sect. 2 and Fig. 1). However, the orbits of the system are in general highly

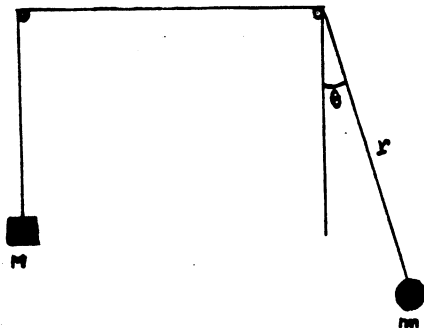


Fig. 1 — SAM : Swinging Atwood's Machine.

(*) Partially supported by CIRIT under grant n° EE88/2.

(**) Partially supported by the grant of the C.G.I.C.T. n° PB86-0351.

complex, as shown by numerical experiments (see [1, 2]). For $\mu = 3$, the system is known to be integrable, and numerical experiments suggest that it is integrable whenever $\mu = 4n^2 - 1$, $n \in \mathbb{N}$ (see Fig. 2).

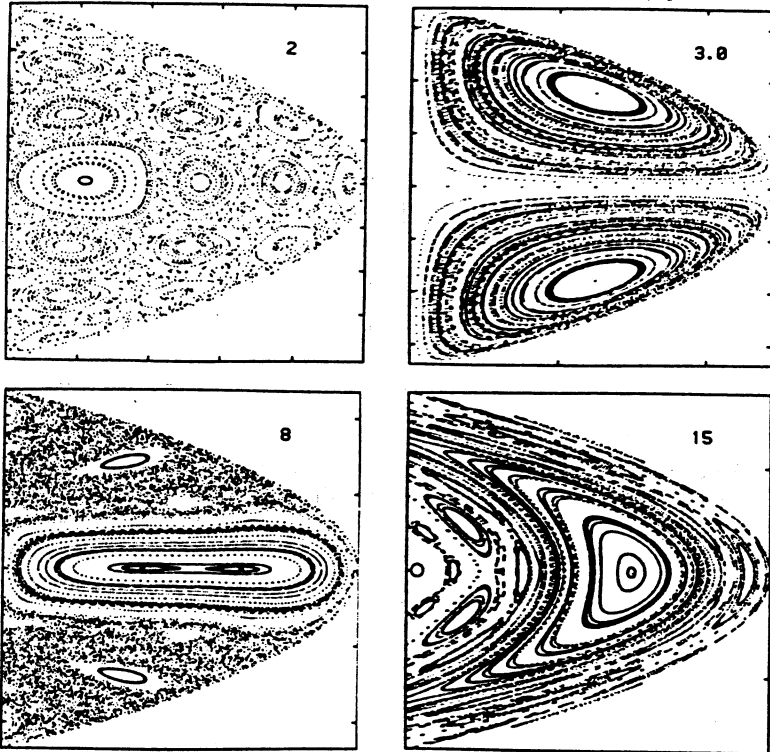


Fig. 2. — Surface of section map (r, \dot{r}) . Cases $\mu = 2$, $\mu = 3$, $\mu = 8$ and $\mu = 15$.

In a previous work (see [3]) we gave a qualitative description of all the SAM orbits for $\mu \in (0, 1)$. In this paper we consider the case $\mu > 1$ and show that there exists a transversal heteroclinic orbit in every energy level (thus, the SAM equations for $\mu = 3$ is one of the few examples of integrable systems with transversal heteroclinic orbits) and that the system is always non-integrable for every μ , except possibly for a discrete set of values in the interval $(1, 3]$, see sections 4 and 3, respectively. This gives a negative answer to the integrability conjecture, but the question remains of explaining why does the system « look » integrable for $\mu = 4n^2 - 1, n > 2$ (see Fig. 2). In fact regular behaviour in non-integrable Hamiltonian systems is not a surprising phenomena when we are dealing with systems which are close to integrable ones, but this is not the case, since the SAM equations are non-integrable for every $\mu > 3$.

In section 5, we study for $\mu = 4n^2 - 1, n \geq 2$, the orbits which pass close to the transversal heteroclinic orbits and show that they remain confined to a small region of their energy levels, which explains why chaotic behaviour is not apparent in a rough numerical experiments. Moreover, we characterize the qualitative behaviour of these orbits, and show that they are formed by sequences of $2n\pi$ direct or retrograde rotations around the origin, separated by motions for which the r -coordinate (radial coordinate) has a well defined extremum at $\theta = \pi$. Although we do not prove the conjugacy of this set of orbits with a shift on a symbolic

complex, as shown by numerical experiments (see [1, 2]). For $\mu = 3$, the system is known to be integrable, and numerical experiments suggest that it is integrable whenever $\mu = 4n^2 - 1$, $n \in \mathbb{N}$ (see Fig. 2).

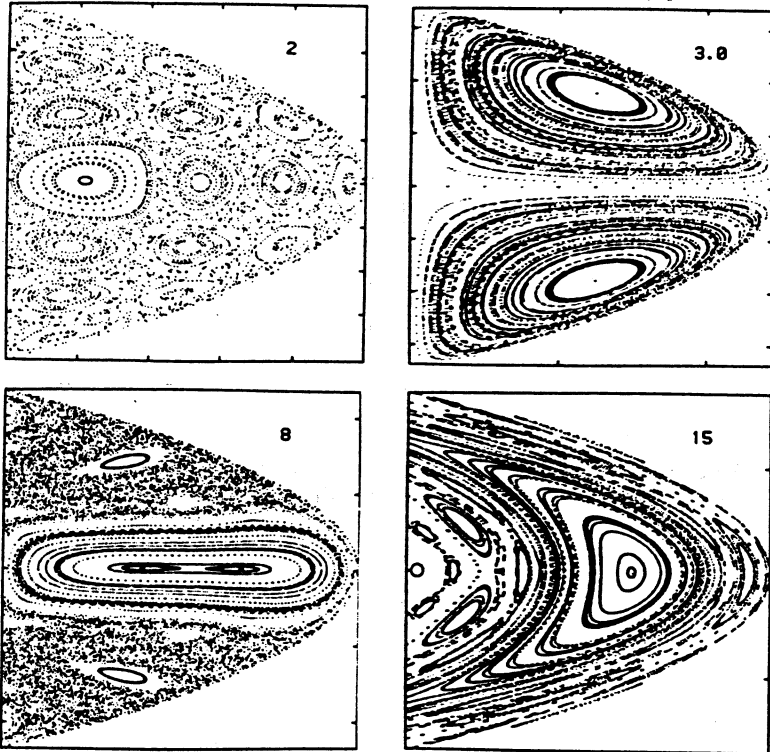


Fig. 2. — Surface of section map (r, \dot{r}) . Cases $\mu = 2$, $\mu = 3$, $\mu = 8$ and $\mu = 15$.

In a previous work (see [3]) we gave a qualitative description of all the SAM orbits for $\mu \in (0, 1)$. In this paper we consider the case $\mu > 1$ and show that there exists a transversal heteroclinic orbit in every energy level (thus, the SAM equations for $\mu = 3$ is one of the few examples of integrable systems with transversal heteroclinic orbits) and that the system is always non-integrable for every μ , except possibly for a discrete set of values in the interval $(1, 3]$, see sections 4 and 3, respectively. This gives a negative answer to the integrability conjecture, but the question remains of explaining why does the system « look » integrable for $\mu = 4n^2 - 1, n > 2$ (see Fig. 2). In fact regular behaviour in non-integrable Hamiltonian systems is not a surprising phenomena when we are dealing with systems which are close to integrable ones, but this is not the case, since the SAM equations are non-integrable for every $\mu > 3$.

In section 5, we study for $\mu = 4n^2 - 1, n \geq 2$, the orbits which pass close to the transversal heteroclinic orbits and show that they remain confined to a small region of their energy levels, which explains why chaotic behaviour is not apparent in a rough numerical experiments. Moreover, we characterize the qualitative behaviour of these orbits, and show that they are formed by sequences of $2n\pi$ direct or retrograde rotations around the origin, separated by motions for which the r -coordinate (radial coordinate) has a well defined extremum at $\theta = \pi$. Although we do not prove the conjugacy of this set of orbits with a shift on a symbolic

alphabet (which in this case would be formed by $+ 2 n \pi$ rotations and $- 2 n \pi$ rotations), the unpredictable nature of these solutions becomes clear, since close initial conditions may determine direct or retrograde rotations.

SAM equations.

The Swinging Atwood's machine is the mechanical system shown in figure 1. The system consists of two masses, M and m , connected by a non extensible string. The mass M is allowed to move only along the vertical direction, while the mass m is allowed to move on a plane, and both masses are subjected to gravity.

In terms of the coordinates (r, θ) shown in figure 1, the total energy equation is

$$E = T + V = \left(\frac{1}{2} (M + m) \dot{r}^2 + \frac{1}{2} m r^2 \dot{\theta}^2 \right) + g r (M - m \cos \theta), \tag{1}$$

where g denotes the acceleration due to gravity. Introducing the generalized momenta $p_r = (M + m) \dot{r}$, $p_\theta = m r^2 \dot{\theta}$, the corresponding Hamiltonian is

$$H(r, \theta, p_r, p_\theta) = \frac{1}{2} \left(\frac{p_r^2}{M + m} + \frac{p_\theta^2}{m r^2} \right) + g r (M - m \cos \theta). \tag{2}$$

Motion will therefore be determined by the Hamilton equations associated to (2),

$$\begin{aligned} \dot{r} &= p_r (M + m)^{-1}, \\ \dot{\theta} &= p_\theta m^{-1} r^{-2}, \\ \dot{p}_r &= p_\theta^2 m^{-1} r^{-3} - g (M - m \cos \theta), \\ \dot{p}_\theta &= - g r m \sin \theta. \end{aligned} \tag{3}$$

3. Integrability.

System (2) is said to be integrable if there exists another complex analytic integral besides the energy.

Consider the canonical change of coordinates given by

$$\begin{aligned} x &= r \sin (A \theta), \\ y &= r \cos (A \theta), \\ p_x &= p_r \sin (A \theta) + r^{-1} A^{-1} \cos (A \theta) p_\theta, \\ p_y &= p_r \cos (A \theta) - r^{-1} A^{-1} \sin (A \theta) p_\theta, \end{aligned} \tag{4}$$

where $A = \left(\frac{m}{(M + m)} \right)^{1/2}$. Then, the dynamics of (2) is equivalent to the dynamics of the Hamiltonian

$$H(x, y, p_x, p_y) = \frac{1}{2} (p_x^2 + p_y^2) + g (m + M) (x^2 + y^2)^{1/2} (M - m \cos (A^{-1} \arctan (x/y))). \tag{5}$$

The kinetic energy term $\frac{1}{2} (p_x^2 + p_y^2)$ is now of the form required to apply Ziglin-Yoshida's

criterion of non-integrability of Hamiltonians with potentials given by homogeneous functions of integer degree (see [4], or [5] for a general review of non-integrability criteria). Moreover, the potential function of (5),

$$V(x, y) = g(m + M)(x^2 + y^2)^{1/2} (M - m \cos(A^{-1} \arctan(x/y))), A = \left(\frac{m}{M + m} \right)^{1/2},$$

is homogeneous of degree $k = 1$. Thus, we have brought the SAM's Hamiltonian (2) to an equivalent Hamiltonian formulation which is in the conditions of Ziglin-Yoshida's criterium.

For homogeneous potentials $V(x, y)$ of degree $k = 1$, this criterium says that if

$$\lambda(c_1, c_2) = \text{trace } V_{xy}(c_1, c_2) \neq \frac{j(j+1)}{2}, \quad j \in \mathbb{N},$$

where V_{xy} is the Hessian matrix of $V(x, y)$ and (c_1, c_2) is a solution of the system

$$c_1 = \frac{\partial V}{\partial x}(c_1, c_2),$$

$$c_2 = \frac{\partial V}{\partial y}(c_1, c_2),$$

then the Hamiltonian $H(x, y, p_x, p_y) = \frac{1}{2}(p_x^2 + p_y^2) + V(x, y)$ is non-integrable.

Computing λ for system (5), we have the following result.

THEOREM 1. — If $\mu = \frac{M}{m} \neq j(j+1)/(j(j+1) - 4)$, for every integer $j > 2$, then system (2) is non-integrable. In particular, if $\mu = \frac{M}{m} \in (0, 1) \cup (3, +\infty)$ then system (2) is non-integrable.

For $\mu = 3$ system (2) is known to be integrable, since an additional analytic integral has been found explicitly in [1] and [2], where it was also conjectured that system (2) should be integrable for every $\mu = 4j^2 - 1$, j integer and greater than 2. This conjecture, to which theorem 1 gives a negative answer, was based on numerical evidence (see Fig. 2). When we are dealing with non-integrable Hamiltonians close to integrable ones, numerical experiments are often misleading, since « most » invariant manifolds (KAM tori and stable and unstable manifolds of invariant one-manifolds) persist in the perturbed system. However, from theorem 1, we see that this is not the case for $\mu = 4j^2 - 1$, $j > 2$. In section 5 we give an explanation for the apparent regularity of the orbits of system (2) when μ takes any of these values.

4. Transversal heteroclinic orbits.

In this section we shall study the existence of transversal heteroclinic orbits, i.e., orbits which lie on the transversal intersection of the stable and the unstable manifolds of two distinct invariant objects and are asymptotic to two equilibrium points. These orbits are usually related to the existence of chaotic dynamics.

Equations (3) are singular at $r = 0$. This singularity is due only to the fact that they are written in polar coordinates, since the potential and its derivatives are regular at $r = 0$. We shall introduce a change of variables and time scale that map the singularity onto a two dimensional torus on the boundary of each energy level, and allows us to extend the flow over this boundary.

Let then $v = p_r(\mu + 1)^{-1/2}$, $u = p_\theta r^{-1}$, $\frac{dt}{d\tau} = mr(\mu + 1)^{1/2}$, with $\mu = M/m$. In terms of new variables, the equations of motion become

$$\begin{aligned} \dot{r} &= rv, \\ \dot{\theta} &= (\mu + 1)^{1/2} u, \\ \dot{v} &= u^2 - gm^2 r (\mu - \cos \theta), \\ \dot{u} &= -uv - gm^2(1 + \mu)^{1/2} r \sin \theta, \end{aligned}$$

where the dot denotes the derivative with respect to the new time scale τ , and the energy relation (2) becomes,

$$\frac{1}{2} (u^2 + v^2) + grm^2(\mu - \cos \theta) = h = \text{Cst.} \tag{7}$$

Letting $r \rightarrow 0$ in (7), we obtain the collision manifold $\Lambda_h = \{(r, \theta, v, u) : r = 0, \theta \in S^1, v^2 = 2h\}$, which lies on the boundary of the energy level I_h given by $I_h = \{(r, \theta, v, u) : (7) \text{ holds}\}$ and represents the singularity $r = 0$.

The flow on Λ_h is given by letting $r \rightarrow 0$ in (6). It is easy to check that the solution on Λ_h are as shown in figure 3: the circles S^+ and S^- are formed by equilibrium points, connected by orbits whose θ -coordinate increases $(\mu + 1)^{1/2} \pi$.

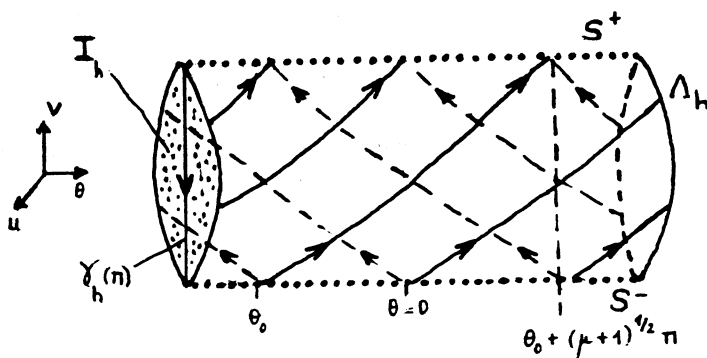


Fig. 3. — The collision manifold Λ , and the phase space $\bar{I}_h = I_h \cup \Lambda$.

Thus, with this regularization, we have introduced in the system two circles of equilibrium points, and compactified the sets I_h where motion take place by extending the flow to their boundary Λ_h .

From (6) it is easy to check that there exist two orbits $\gamma(\theta_0)$, $\theta_0 = 0, \pi$, in every energy level I_h , $h > 0$, such that $\theta(\tau) \equiv \theta_0$, $u(\tau) \equiv 0$ and $r(\tau)$ tends to $r = 0$ when $\tau \rightarrow +\infty$ and when $\tau \rightarrow -\infty$. Therefore, $\gamma(\theta_0)$, $\theta_0 = 0, \pi$, is an heteroclinic orbit since it tends to an equilibrium point on S^+ (resp. on S^-) when $\tau \rightarrow -\infty$ (resp. $\tau \rightarrow +\infty$). We shall say that $\gamma(\theta_0)$, $\theta_0 = 0, \pi$, is transversal in I_h if the stable manifold of S^- , $W^s(S^-)$, and the unstable manifold of S^+ , $W^u(S^+)$, intersect transversally along $\gamma(\theta_0)$.

Since S^+ and S^- are normally hyperbolic invariant circles, $W^u(S^+)$ and $W^s(S^-)$ exist and are two-dimensional smooth manifolds (see [6]). In order to study the transversality of $\gamma(\theta_0)$, $\theta_0 = 0, \pi$, we must know the geometry of $W^{u,s}(S^{\pm})$ in a neighbourhood of

$\gamma(\theta_0)$ at least to first order. From (6), the normal first order variational equations in a neighbourhood of $\gamma(\theta_0)$ are

$$\begin{aligned} \dot{\theta} &= (\mu + 1)^{1/2} u, \\ \dot{u} &= -v_0(\tau) u - gm^2(\mu + 1)^{1/2} r_0(\tau) \theta \cos(\theta_0), \end{aligned} \tag{8}$$

where $r_0(\tau)$, $v_0(\tau)$ are the solutions of (6) along $\gamma(\theta_0)$ that verifies $v_0(0) = 0$. Then, the angle $\varphi^u(\tau)$ that the intersection of $W^u(S^+)$ with the plane $v = v_0(\tau)$ forms with the $u = 0$ axis on this plane is

$$\varphi^u(\tau) = \arctan \frac{u(\tau)}{\theta(\tau)},$$

with $\theta(\tau)$, $u(\tau)$ solutions of (8) such that $\lim_{\tau \rightarrow -\infty} u(\tau) = 0$. Hence, $\varphi^u(\tau)$ is the solution of

$$\dot{\varphi}(\tau, \varphi) = -gm^2(1 + \mu)^{1/2} \cos \theta_0 r_0(\tau) \cos^2 \varphi - v_0(\tau) \sin \varphi \cos \varphi - (\mu + 1)^{1/2} \sin^2 \varphi \tag{9}$$

with asymptotic condition $\lim_{\tau \rightarrow -\infty} \varphi(\tau) = 0$.

It is easy to check numerically that for $\theta_0 = \pi$, $\varphi^u(0) \in (0, \pi/2)$ for every $\mu > 1$. This result may also be proved analytically using the techniques introduced in [7]. Similarly, the angle $\varphi^s(\tau)$ that the intersection of $W^s(S^-)$ with the plane $v = v_0(\tau)$ forms with the $u = 0$ axis on this plane is the solution of (9) with asymptotic condition $\lim_{\tau \rightarrow +\infty} \varphi^s(\tau) = 0$,

and, if $\theta_0 = \pi$, $\varphi^s(0) \in (-\pi/2, 0)$ for every $\mu > 1$. Hence, the intersection of $W^u(S^+)$ and $W^s(S^-)$ along $\gamma(\pi)$ is transversal at $(r_0(0), \pi, 0, 0)$. See figure 4.

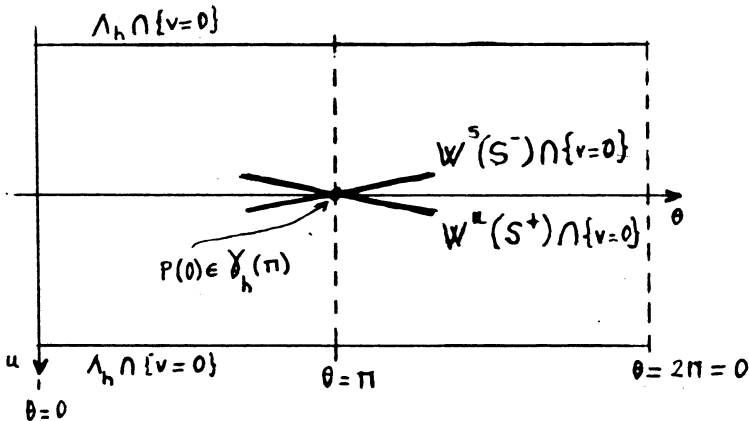


Fig. 4. — Local behaviour of $W^u(S^+) \cap \{v = 0\}$ and $W^s(S^-) \cap \{v = 0\}$.

Now suppose that for some τ^* ,

$$\varphi^u(\tau^*) - \varphi^s(\tau^*) = k\pi, \quad k \in \mathbb{Z}.$$

Let then $v = p_r(\mu + 1)^{-1/2}$, $u = p_\theta r^{-1}$, $\frac{dt}{d\tau} = mr(\mu + 1)^{1/2}$, with $\mu = M/m$. In terms of the new variables, the equations of motion become

$$\begin{aligned} \dot{r} &= rv, \\ \dot{\theta} &= (\mu + 1)^{1/2} u, \\ \dot{v} &= u^2 - gm^2 r (\mu - \cos \theta), \\ \dot{u} &= -uv - gm^2(1 + \mu)^{1/2} r \sin \theta, \end{aligned}$$

where the dot denotes the derivative with respect to the new time scale τ , and the energy relation (2) becomes,

$$\frac{1}{2} (u^2 + v^2) + grm^2(\mu - \cos \theta) = h = \text{Cst.} \tag{7}$$

Letting $r \rightarrow 0$ in (7), we obtain the collision manifold $\Lambda_h = \{(r, \theta, v, u) : r = 0, \theta \in S^1, v^2 + u^2 = 2h\}$, which lies on the boundary of the energy level I_h given by $I_h = \{(r, \theta, v, u) : (7) \text{ holds}\}$ and represents the singularity $r = 0$.

The flow on Λ_h is given by letting $r \rightarrow 0$ in (6). It is easy to check that the solution on Λ_h are as shown in figure 3: the circles S^+ and S^- are formed by equilibrium points, connected by orbits whose θ -coordinate increases $(\mu + 1)^{1/2} \pi$.

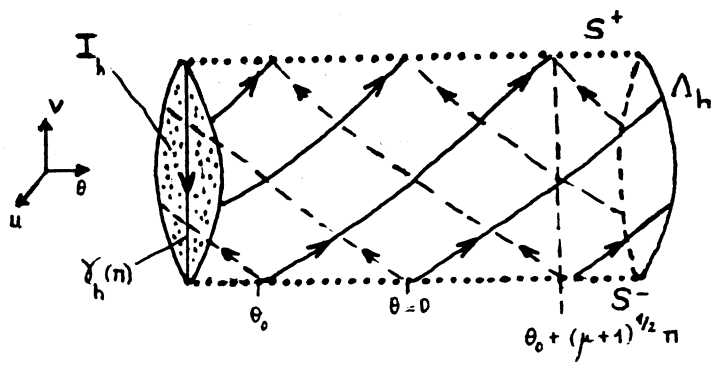


Fig. 3. — The collision manifold Λ , and the phase space $\bar{I}_h = I_h \cup \Lambda$.

Thus, with this regularization, we have introduced in the system two circles of equilibrium points, and compactified the sets I_h where motion take place by extending the flow to their boundary Λ_h .

From (6) it is easy to check that there exist two orbits $\gamma(\theta_0)$, $\theta_0 = 0, \pi$, in every energy level I_h , $h > 0$, such that $\theta(\tau) \equiv \theta_0$, $u(\tau) \equiv 0$ and $r(\tau)$ tends to $r = 0$ when $\tau \rightarrow +\infty$ and when $\tau \rightarrow -\infty$. Therefore, $\gamma(\theta_0)$, $\theta_0 = 0, \pi$, is a heteroclinic orbit since it tends to an equilibrium point on S^+ (resp. on S^-) when $\tau \rightarrow -\infty$ (resp. $\tau \rightarrow +\infty$). We shall say that $\gamma(\theta_0)$, $\theta_0 = 0, \pi$, is transversal in I_h if the stable manifold of S^- , $W^s(S^-)$, and the unstable manifold of S^+ , $W^u(S^+)$, intersect transversally along $\gamma(\theta_0)$.

Since S^+ and S^- are normally hyperbolic invariant circles, $W^u(S^+)$ and $W^s(S^-)$ exist and are two-dimensional smooth manifolds (see [6]). In order to study the transversality of $\gamma(\theta_0)$, $\theta_0 = 0, \pi$, we must know the geometry of $W^{u,s}(S^{\pm})$ in a neighbourhood of

Then, we have

$$\begin{aligned} (d(\varphi^u(\tau) - \varphi^s(\tau))/d\tau)(\tau^*) &= -gm^2(\mu + 1)^{1/2} \cos \theta_0 r_0(\tau)(\cos^2 \varphi^u(\tau^*) - \cos^2 \varphi^s(\tau^*)) \\ &\quad - v_0(\tau)(\sin \varphi^u(\tau^*) \cos \varphi^u(\tau^*) - \sin \varphi^s(\tau^*) \cos \varphi^s(\tau^*)) \\ &\quad - (\mu + 1)^{1/2} (\sin^2 \varphi^u(\tau^*) - \sin^2 \varphi^s(\tau^*)) = 0. \end{aligned}$$

Hence, if $W^u(S^+)$, $W^s(S^-)$ intersect transversally at one point of $\gamma(\pi)$, they intersect transversally along $\gamma(\pi)$, and we have proved the following.

THEOREM 2. — For every $\mu \in (1, +\infty)$ and $h > 0$, $\gamma_h(\pi)$ is a transversal heteroclinic orbit.

Since transversal heteroclinic orbits usually give rise to chaotic dynamics, one should expect system (2) to be non-integrable for every $\mu > 1$ and this is indeed confirmed by Theorem 1, with the possible exception of a discrete set of values of μ . Actually, the integrable case $\mu = 3$ is one of the few examples of integrable systems with transversal heteroclinic orbits; other examples of this pathological feature have been constructed in [8] and [9].

In the following section, we shall use the results obtained so far to describe qualitatively the behaviour of the orbits of (2) when $\mu = 4n^2 - 1$, $n > 2$, and to explain why does the system «look» integrable for these values of μ (see Fig. 2 again).

5. Dynamical description.

When $\mu \in (0, 1)$ and $h < 0$, the phase of constant energy h , I_h (resp. \bar{I}_h), is an open solid ellipsoid (resp. closed solid ellipsoid) and the boundary corresponds to the infinity manifold (which replaces the singularity $r = +\infty$). In these cases it is possible to describe the qualitative behaviour of the global flow on I_h , see [3]: every solution, with the exception of the homothetic orbits, is doubly asymptotic to infinity, crossing the $\theta = 0$ axis a finite or infinite number of times according to whether $\mu \in (0, 1/17)$ or $\mu \in (1/17, 1)$.

The purpose of this section is, using the knowledge of the flow on the collision manifold and the existence of the transversal heteroclinic orbit $\gamma_h(\pi)$ (see Theorem 2), to show the behaviour of the solutions of SAM which are close to this heteroclinic orbit when $\mu \in (1, +\infty)$ and $h > 0$. For dynamical description of the solutions we shall use symbolic dynamics; first we shall define the motions (or symbols).

Let $\bar{\theta} \in S^1$ and denote by $\bar{I} = [\bar{\theta} - \delta, \bar{\theta} + \delta]$, for some $\delta > 0$. We say that a solution of (6), $p(\tau) = (r(\tau), \theta(\tau), v(\tau), u(\tau))$, $\tau \in [\tau_1, \tau_2]$, realizes a motion of type $\bar{\theta}$, and we represent it by $\bar{\theta}$, when $\theta(\tau) \in \bar{I}$ for every $\tau \in [\tau_1, \tau_2]$ and $r(\tau)$, $\tau \in [\tau_1, \tau_2]$, has exactly one relative maximum. See figure 5.

We shall represent by $(A, s(k), B)$, A and B are motions of type $\bar{\theta}_1$ and $\bar{\theta}_2$ respectively, and $s(k) \in \{k, -k\}$ where $k \in \mathbb{N}$, the set of solutions of (6) $p(\tau) = (r(\tau), \theta(\tau), v(\tau), u(\tau))$, $\tau \in [\tau_1, \tau_4]$, such that satisfy: $\exists \tau_2, \tau_3, \tau_1 < \tau_2 < \tau_3 < \tau_4$, where:

$p(\tau)$, $\tau \in [\tau_1, \tau_2]$, realizes a motion of type A ,
 $p(\tau)$, $\tau \in [\tau_3, \tau_4]$, realizes a motion of type B , and
 $p(\tau)$, $\tau \in [\tau_2, \tau_3]$, verifies $\theta'(\tau) \neq 0$, $r(\tau)$ has only one relative minimum, and if $s(k) = k$ (resp. $s(k) = -k$) then $\theta(\tau)$, $\tau \in [\tau_2, \tau_3]$, increases (resp. decreases) $2k\pi + (\bar{\theta}_2 - \bar{\theta}_1)$. In figure 6 we have represented the orbits which realizes $(\bar{\theta}_1, 2, \bar{\theta}_2)$ and $(\bar{\theta}_1, -2, \bar{\theta}_2)$.

Let $\ell, k \in \mathbb{N}$. We shall define $T_\ell(k)$ as the sequence of length ℓ of motions of rotation type

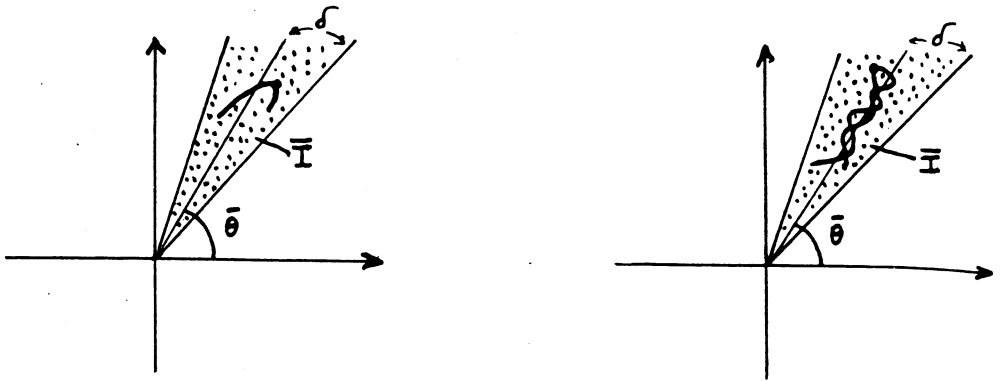


Fig. 5. — Motions of type $\bar{\theta}$ (on the positions plane of polar coordinates (r, θ)).

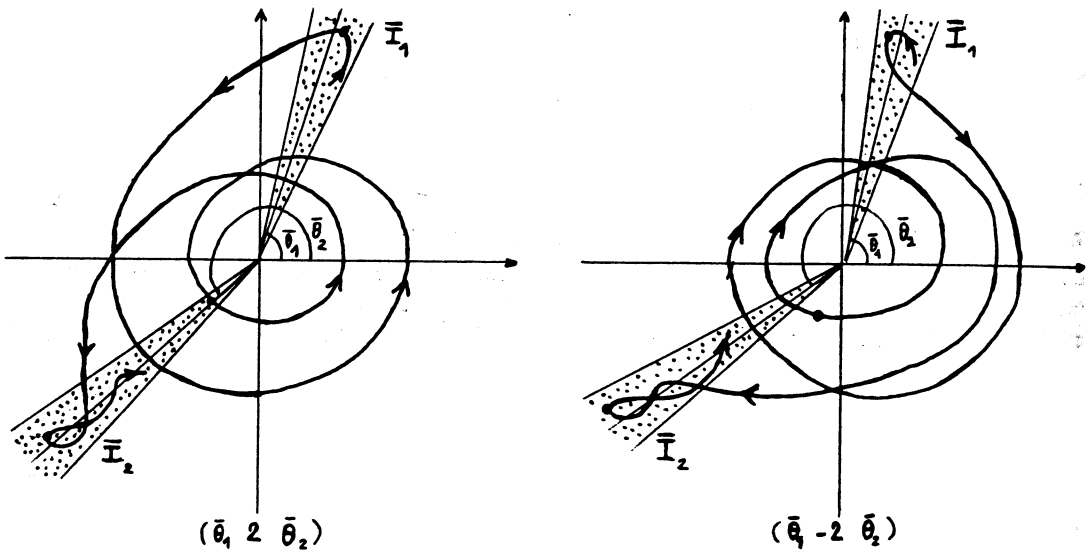


Fig. 6. — Solutions which realize $(\bar{\theta}_1, 2, \bar{\theta}_2)$ and $(\bar{\theta}_1, -2, \bar{\theta}_2)$ here we have draw the projections on the positions plane of polar coordinate $r(\theta)$.

$k, T_\ell(k) = (\bar{\theta}_0, s_0(k), \bar{\theta}_1, s_1(k), \dots, \bar{\theta}_{\ell-1}, s_{\ell-1}(k), \bar{\theta}_\ell)$, where $\bar{\theta}_i \in S$ and $s_i(k) \in \{k, -k\}$ for $i = 0, \dots, \ell$. A solution $p(\tau)$ of (6) realizes $T_\ell(k)$ if it belongs to the sets $(\bar{\theta}_0, s_0(k), \bar{\theta}_1), (\bar{\theta}_1, s_1(k), \bar{\theta}_2), \dots, (\bar{\theta}_{\ell-1}, s_{\ell-1}(k), \bar{\theta}_\ell)$ as time increases.

Our fundamental result concerning the dynamical description of the orbits of (6) is stated in the following theorem.

THEOREM 3. — Suppose $\mu = 4k^2 - 1, k \in \mathbb{N}$, and $h \geq 0$. Then, given $\ell \in \mathbb{N}$, there exists a neighbourhood U of $p(0) \in \gamma_h(\pi) \cap \{v = 0\}$ such that for every $p \in U \setminus W^s(S^-)$ the orbit through p realizes a sequence $T_\ell(k)$ with $\bar{\theta}_i = \pi$ for $i = 0, \dots, \ell$.

Proof. — Consider a neighbourhood N of $\gamma_h(\pi)$ in the plane $\{v = 0\}$ in I_h . According to the

results of the previous section, the manifolds $W^u(S^+)$, $W^s(S^-)$ intersect this neighbourhood as shown in figure 7, defining the four open sectors S_1, S_2, S_3, S_4 .

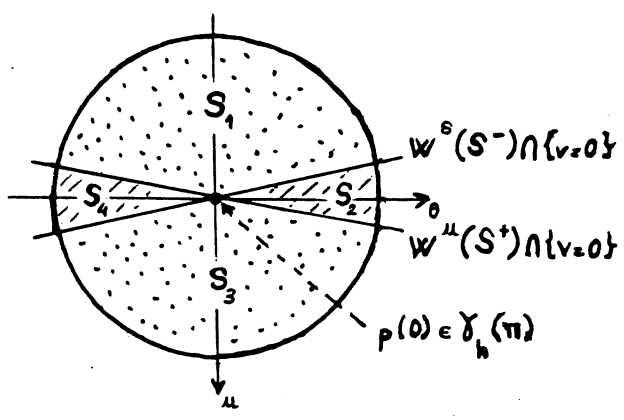


Fig. 7. — Dynamical behaviour of the solutions in a neighbourhood of $p(0) \in \gamma_h(\pi)$, when $\mu = 4k^2 - 1$, $k \in \mathbb{N}$, and $h > 0$. The points of the open sector S_1, S_2, S_3, S_4 realize $(\pi, -k, \pi, -k, \pi)$, $(\pi, -k, \pi, k, \pi)$, (π, k, π, k, π) , $(\pi, k, \pi, -k, \pi)$, respectively.

If N is small enough, the orbits through N will follow close to the homothetic orbit until they reach a neighbourhood of the collision manifold, and then they will follow closely to the flow on Λ . Since by hypothesis $\mu = 4k^2 - 1$, the θ coordinate of the orbits on Λ changes by $2k\pi$ between S^+ and S^- (see Fig. 2) and so this will take them again to a neighbourhood of $\gamma_h(\pi)$. Following this way the orbits through the boundary of N in forward or backward time, we conclude that the forward and backward image of N by the flow is another neighbourhood N' of $\gamma_h(\pi) \cap \{v = 0\}$, divided also into four sectors S'_1, S'_2, S'_3 and S'_4 by the manifolds $W^u(S^+)$, $W^s(S^-)$.

Moreover, the sectors $S_i, i = 1 \div 4$, determine the type of motion that an orbit in N may realize. For instance, it is clear from figure 3 and figure 4 that an orbit through p in N will realize, as time runs forward, an orbit of the form (π, k, π) or $(\pi, -k, \pi)$ according to whether p lies on one side or another of $W^s(S^-)$. Similarly, the behaviour when time runs backwards is also determined by the sectors $S_i, i = 1 \div 4$, in fact, depending on which side of $W^u(S^+)$. Thus we obtain the table of figure 7, and the result follows.

The reason why it is possible to make the large time qualitative predictions of the preceding theorem is that for $\mu = 4k^2 - 1, k \in \mathbb{N}$, the flow on the collision manifold is such that the orbits that start close to the heteroclinic orbit $\gamma_h(\pi)$ will always stay close either to $\gamma_h(\pi)$ or to Λ . This explains also why the system seems to be integrable in numerical experiments. In fact, the chaotic orbits associated to the transversal intersection of $W^u(S^+)$ and $W^s(S^-)$ at $\gamma_h(\pi)$ will remain confined to a neighbourhood of $\gamma_h(\pi)$ and of Λ on each energy level. Therefore, it will be very hard to detect them in a numerical computation of the Poincaré map of the $\theta = 0$ plane in I_h , since all these orbits will correspond to points which pass very close to $r = 0, v = 0$.

References

- [1] TUFILLARO N., Integrable motion of a swinging Atwood's machine, *Am. J. Phys.* **54** (1986) 142-143.
- [2] TUFILLARO N., Motions of a swinging Atwood's machine, *J. phys. France* **46** (1985) 1495-1500.
- [3] CASASAYAS J., TUFILLARO N., NUNES A., Infinity Manifold of the Swinging Atwood's Machine, *Eur. J. Phys.* **10** (1989) 173-177.
- [4] YOSHIDA H., A criterion for the non existence of an additional integral in Hamiltonian systems with homogeneous potential, *Physica* **29D** (1987) 128-142.
- [5] ZIGLIN S. L., YOSHIDA H. *et al.*, *Phys. Rep.* **180** (1989) 160.
- [6] HIRSCH M., PUGH C., SHUB M., Invariant manifolds, *Lecture Notes Math.* No. 583 (Springer-Verlag) 1977.
- [7] CASASAYAS J., LLIBRE J., Qualitative analysis of the anisotropic Kepler problem, *Memoirs of the AMS* vol. **52** (1984) No. 312.
- [8] WIGGINS S., *Global Bifurcations and Chaos* (Springer-Verlag) 1988.
- [9] DEVANEY R., Transversal homoclinic orbits in an integrable system, *Am. J. Math.* **100**, pp. 631-642.